Hindawi
International Journal of Chemical Engineering
Volume 2023, Article ID 3245973, 20 pages
https://doi.org/10.1155/2023/3245973

Research Article

Analytical Steady-State Model for the Free Radical Solution Copolymerization of Acrylonitrile and Vinyl Acetate and Their Charge-Transfer Complex in a Continuous Stirred Tank Reactor

Oscar Meza-Díaz,[1] Juan-Carlos Tapia-Picazo,[1] Adrian Bonilla-Petriciolet,[1] Gabriel Luna-Bárcenas,[2] Daniel Alcalá-Sánchez,[1] José-Enrique Jaime-Leal,[1] and Pedro-Jesús Herrera-Franco[3]

[1]*Tecnológico Nacional de México, Instituto Tecnológico de Aguascalientes, Aguascalientes 20256, Mexico*
[2]*Cinvestav-Querétaro, Querétaro 76230, Mexico*
[3]*Yucatan Scientific Research Center, Mérida, Yucatán 97200, Mexico*

Correspondence should be addressed to Juan-Carlos Tapia-Picazo; tapiajc@hotmail.com

Received 14 July 2022; Revised 30 January 2023; Accepted 17 March 2023; Published 27 May 2023

Academic Editor: Achim Kienle

In this study, a mathematical model of the copolymerization of AN-VA in a continuous stirred tank reactor (CSTR) was developed considering charge-transfer complexes (CTCs). CTC formation between acrylonitrile (AN) and vinyl acetate (VA) was demonstrated using UV-VIS spectrophotometry and molecular orbital theory. The rate constants and equilibrium constants of the complexes were calculated from a model of the simultaneous participation of complexes and free monomers and the molar ratio method. Furthermore, the participation of CTCs in propagation was included because of their high reactivity. All the simultaneous equations defined to analyze the reactor parameters were analytically solved, and the results of the model were in terms of operative variables such as monomer conversion, average molecular weight, and the mole fraction of monomer 2 (i.e., VA) in the polymer formed. The results of the predictions of the developed model were compared with the experimental data for validation. This prediction was also compared with the reactor model solution without considering the CTC, which showed deviations that were more significant than those of the CTC model. These results represent a quantitative way to analyze the order of magnitude of the impact of the formation of the complexes in the analyzed polymerization system.

1. Introduction

Polymerization system modeling is difficult because of its high complexity. Nevertheless, the mathematical model is a powerful tool for studying and understanding the phenomena involved in the polymerization process and improving the physical properties and features of polymers and their manufacturing processes.

Reactive systems of acrylonitrile (AN) and vinyl acetate (VA) have been used to prepare low-cost acrylic fibers and carbon fiber precursor fibers. AN is widely used as a raw material for the production of various products used in everyday life, such as stamens, auto parts, plastics, and synthetic gum. Polyacrylonitrile (PAN) is also a very common polymer; for example, it is used as a cathode in batteries [1], precursor of textile fibers [2, 3], and high-efficiency fibers (i.e., carbon fibers) because of its exceptional mechanical properties, attributed to its aligned molecular structure [4]. Furthermore, VA can be employed with AN to obtain a copolymer whose solubility facilitates extrusion and alters the shape and characteristics of the acrylic fiber [5]. VA can modify the properties of polymers owing to its unsaturated structure.

In this direction, it is convenient to indicate that several techniques can be used to perform copolymerization reactions. Suspension and solution polymerizations are the

most widely used methods because of their high purity, easy temperature control, and narrow polydispersity. The solution polymerization technique involves the action of a solvent along with other reactive species, such as free monomers, oligomers, and charge-transfer complexes.

The charge-transfer complex (CTC) is a chemical compound derived from or composed of reagents that can be present in different reaction systems and exhibits interesting behavior over the polymer chain structure and the reactivity of all reactive species involved in polymerization.

In the characterization of polymers, it is possible to use spectrophotometric analysis techniques. Several reactive species detected by these techniques, which had not been usually considered in the study of polymerization reactions because their existence has not been recognized, began to be included to describe their presence in the reaction of polymers and to explain several phenomena observed during the reaction. Such is the case of CTCs, and when verifying that their formation was given by several monomers, studies began to be carried out and mathematical models were developed that made it possible to explain that certain characteristics of polymers (e.g., the alternate structure of the polymer chain) were due to the presence of complexes. Rivero and Etchechury [6] have discussed the role of CTCs in the polymerization process, considering the propagation step in which the CTC takes part due to high reactivity. They proposed a terpolymerization model that included CTCs in the terpolymerization process using vinyl chloride, vinyl acetate, and maleic anhydride. Rao et al. [7] studied the methyl methacrylate complex and proposed that the participation of CTCs in the initiation step significantly affects the conversion and average molecular weight. Garra et al. [8] and Wang et al. [9] considered CTCs in the initiation step as initiators of photopolymerization reactions.

In this study, an analytical solution was obtained for the model of free radical solution copolymerization in a continuous stirred tank reactor (CSTR). For the case of AN-VA systems, CTC formation was considered and included in the copolymerization process. With the incorporation of CTCs, a new reaction mechanism has been proposed, which details how polymerization occurs. This represents an excellent alternative for improving the prediction of the properties and characteristics of polymers from mathematical models, which allow the design of new and better acrylic materials and carbon fiber precursors, as in this case. The formation of CTCs between AN and VA was corroborated and included in the propagation steps. Kinetic constants (i.e., propagation rate constants) were determined. Finally, a parametric analysis of this model was carried out, and it was validated by experimental copolymerization results.

2. Experimental Section

2.1. Materials. Acrylonitrile (>99%, Aldrich), vinyl acetate (>99%, Aldrich), ammonium persulfate (99.3%, J. T. Baker), and N, N-dimethylformamide (99.97% J. T. Barker) were used as received.

2.2. Charge-Transfer Complex Formation and Its Verification. A Genesys Thermo Scientific spectrophotometer (series 840-208100), with a wavelength range of 190–1100 nm and an accuracy of ±1.0 nm, was used to determine the formation of CTCs.

As indicated, CTCs are chemical species that are formed between two monomers, one electropositive and the other electronegative, which are compounds joined by van der Waals forces, and charge transfer occurs towards an orbital of the electronegative compound. In this case, the electropositive monomer was acrylonitrile (AN), whereas the electronegative compound was vinyl acetate (VA). The mechanism of complex formation is shown in Figure 1.

CTC formation was verified using the technique proposed by Olson and Butler [10]. This method consists of obtaining the UV-VIS absorbance spectra of solutions of two monomers that will form the CTC individually at a defined concentration and their mix. The absorbance spectra of the mixture were compared with those of the individual monomers, and if there was an increase in the absorbance of the mixture with respect to monomers, it was attributed to the formation of a CTC due to interactions between the electron acceptor and donor, creating a new structure where the energy gap is lower than that of the donor and acceptor [9].

2.3. Experimental Determination of CTC Formation Equilibrium Constants. The formation equilibrium constants of the complexes were obtained using the UV-VIS method, called the molar ratio reported by Skoog et al. [11]. This method consists of mixing the monomer electron acceptor with the donor that will form the CTC, varying the "monomer donor concentration" (C_L), and keeping constant the "monomer acceptor concentration" (C_M). The objective of this technique is to appreciate the "absorbance change" (ΔA) as a function of the monomer donor concentration. Finally, the obtained experimental data are adjusted to equation (1), and the equilibrium constant is calculated from

$$\frac{b}{\Delta A} = \frac{1}{\Delta\varepsilon C_M} + \left(\frac{1}{\Delta\varepsilon C_M K_f}\right) \frac{1}{C_L}, \quad (1)$$

where b, $\Delta\varepsilon$, and K_f are the cell path length, change in molar absorptivity, and CTC formation equilibrium constant, respectively.

2.4. Estimation of CTC Propagation Rate Constants. Polymerization reactions of AN with VA were performed to determine the CTC propagation constant rate. In the reaction system, AN-VA feed monomer ratios of 4.0 pp%–15.0 pp% were used to determine the overall polymerization rate for 15, 30, 45, and 60 min at 50°C. The obtained copolymers were washed several times with deionized water and dried to a constant mass. Copolymer conversion was determined by the ratio of the monomers in the feed to the total mass of the copolymer. The copolymer composition was obtained using the infrared method by Mas-Gilbert et al.

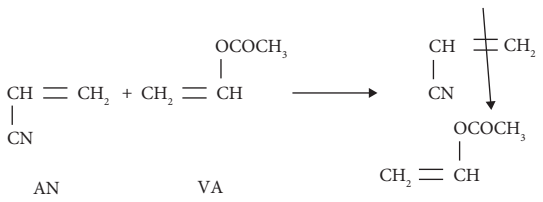

Figure 1: Complex formation between acrylonitrile and vinyl acetate.

[12], where an FTIR Thermo Scientific Nicolet iS10 FTIR spectrometer was applied. The average molecular weight was obtained by viscosity using an Ubbelohde viscometer and the Mark–Houwink equation with the parameters of N, N-dimethylformamide and AN at 25°C.

2.5. Continuous Stirred Tank Reactor Experiment. The polymerization reactions were carried out in a 100 mL experimental reactor heated in a thermal bath at a constant temperature of 50°C. The monomers (AN and VA), initiator (ammonium persulfate), and solvent (N, N-dimethylformamide) were fed to the reactor using a peristaltic pump, and the reactor exit was fed by the overflow principle. The fluxes were established until a steady state was reached with residence times of 20, 30, 45, and 60 min. The obtained copolymers were characterized in terms of their conversion, molecular weight, and composition. The copolymer properties were determined in the same manner as the conversion, molecular weight, and composition, as described in Section 2.4.

3. Results and Discussion

3.1. Formation of CTC Complexes. In this case of study, the donor was AN and VA was the acceptor because the oxygen atoms in the structure of VA are more electronegative than carbon (C) and hydrogen (H) atoms, allowing the attraction of electrons to VA. According to the theory of molecular orbitals, the acceptor has the lowest unoccupied molecular orbital (LUMO) and the donor has the highest occupied molecular orbital (HOMO). When the acceptor and donor are mixed, they create a structure with an energy gap between the LUMO and HOMO that is smaller than that between the donor and acceptor monomers [8]. Therefore, the increase in the absorbance spectra of the mixtures was due to CTC formation.

Various solutions were prepared for AN and VA, with different concentrations of VA (4.0%–15.0% mass feeding) and the rest of AN. Figure 2 shows the absorbance spectra of the copolymers in the 294–400 nm wavelength range [10]. It can be observed that the absorbance at 294 nm increased with the AN concentration.

3.2. Estimation of CTC Propagation Rate Constants. The rate constant of CTCs was obtained with the model for the simultaneous participation of free monomers and the complexes, which was proposed by Braun and Hu [13]. This approach to obtain the CTC propagation rate constants is an approximate method in which the experimental data are fitted to linear models to calculate the numerical values of the rate constants.

The sum of contributions of free monomers (V_f) (equation (2) and CTC (V_{CT}) (equation (3)) is given as a result of the equation of the overall copolymerization rate (V_{br}) (equation (4)). The terms of $A(X)$ and $F(X)$ are constants for a certain monomer ratio X = [AN]/[VA] and feed initiator concentration. Equation (5) defines $F(X)$ as a function of the CTC rate constant, copolymerization propagation rate, and CTC formation equilibrium constant. Experiments were performed to obtain $A(X)$ and $F(X)$ and finally to calculate k_{1C1} and k_{2C1} (i.e., CTC rate constants) from equation (5):

$$V_f = A(X)[M_1], \tag{2}$$

$$V_{CT} = A(X)F(X)[M_1]^2, \tag{3}$$

$$\frac{V_{br}}{[M_1]} = A(X) + A(X)F(X)[M_1], \tag{4}$$

$$\frac{F(X)}{K_f} = \frac{k_{1C1}}{k_{p12}} + \frac{k_{2C1}}{k_{p21}}X. \tag{5}$$

The results of the experiments are shown in Figures 3 and 4, where each graph contains a straight-line equation for obtaining $A(X)$ and $F(X)$ values. Those values were used for calculating the $F(X)/K_f$ ratio. Note that K_f is the CTC formation equilibrium constant and was determined experimentally according to the method described in Section 2.3. The results are shown in Table 1 and plotted in Figure 5.

According to equation (5) and Figure 4, the following relative reactivities were calculated: (k_{1C1}/k_{p12}) = 14.965, and (k_{2C1}/k_{p21}) = 6.608. These values indicate that CTCs are 15 times more reactive against free AN and 7 times more reactive than free VA. Finally, the CTC propagation rate constants were calculated using k_{p12} and k_{p21}, obtaining $k_{p121} = 1.29 \times 10^6\ \mathrm{L \cdot mol \cdot s^{-1}}$ and $k_{p112} = 7.81 \times 10^5\ \mathrm{L \cdot mol \cdot s^{-1}}$.

3.3. Description of the Reaction Mechanism. The modeling of polymerization reactions generally focuses on describing the reaction evolution in terms of monomer conversion and molecular weights. In this case, the free radical solution polymerization (SP) mechanism is used to consider each step of the reaction mechanism and chain transfer terms to the solvent in the termination step, which is an important characteristic of SP.

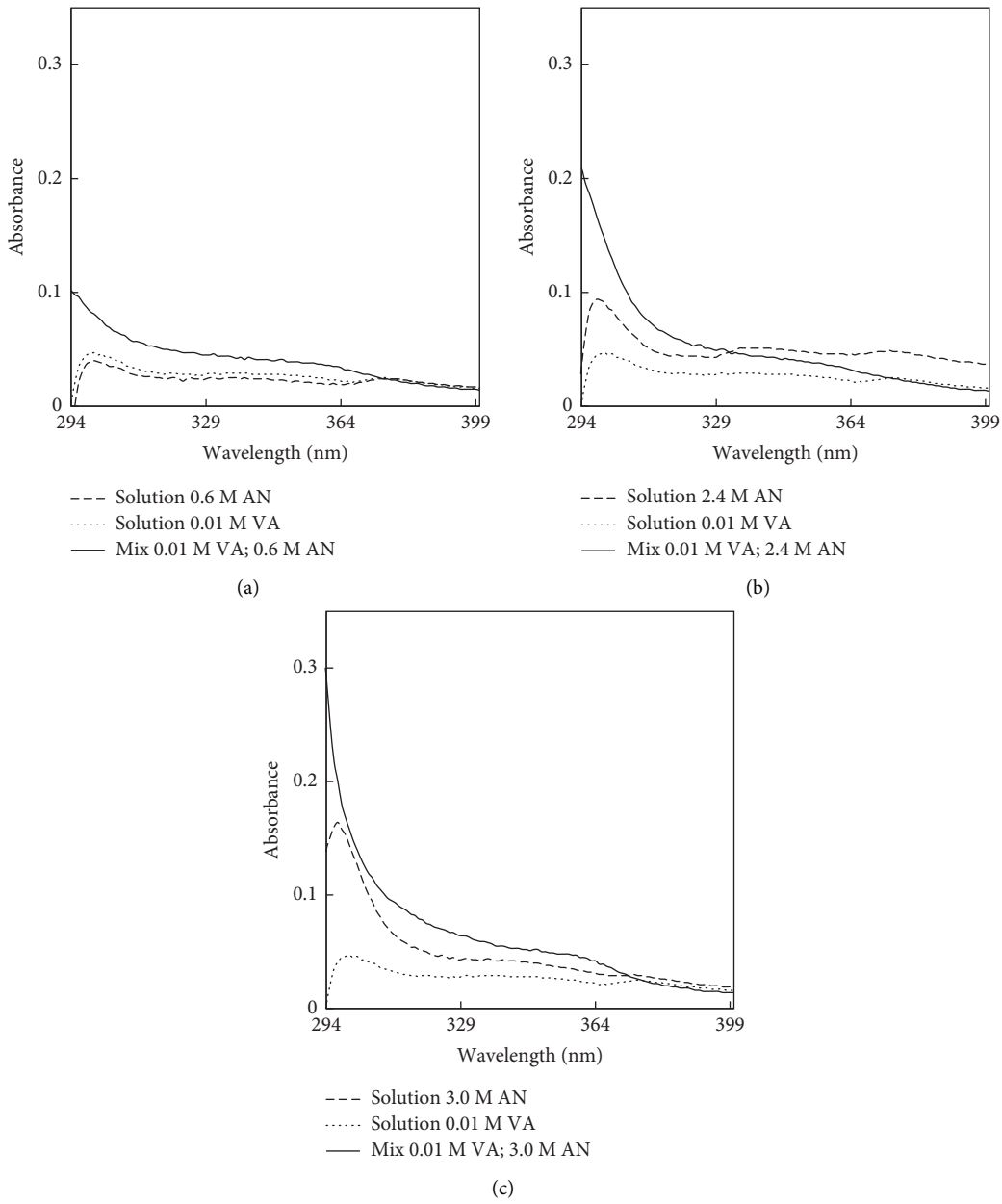

Figure 2: Absorbance spectra of AN, VA, and their mixture. In all the experiments, VA concentration remained constant at 0.01 M AN concentration: (a) 0.6 M, (b) 2.4 M, and (c) 3.0 M.

Equations (6)–(22) are common expressions of the copolymerization free radical mechanism considering the participation of free monomers and the charge-transfer complex [6].

3.3.1. Initiation

$$I_2 \xrightarrow{kd} 2I^{\cdot}, \tag{6}$$

$$I^{\cdot} + M_1 \xrightarrow{ki1} P^{\cdot}_{1,0}, \tag{7}$$

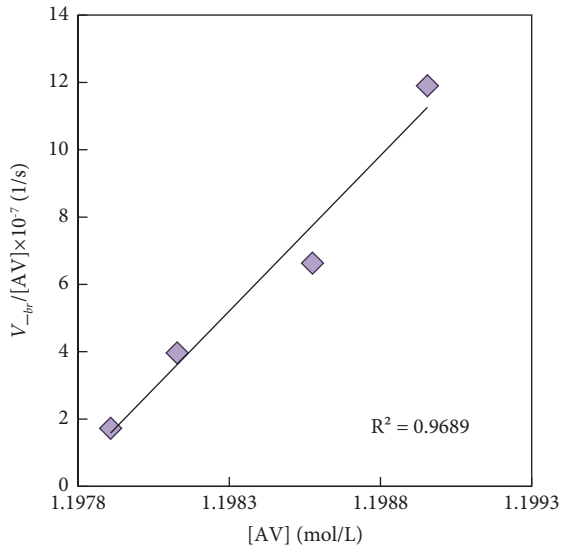

Figure 3: V_{br}/[VA] versus [VA] in dimethylformamide at X = [AN]/[VA] = 3.12 at 50°C.

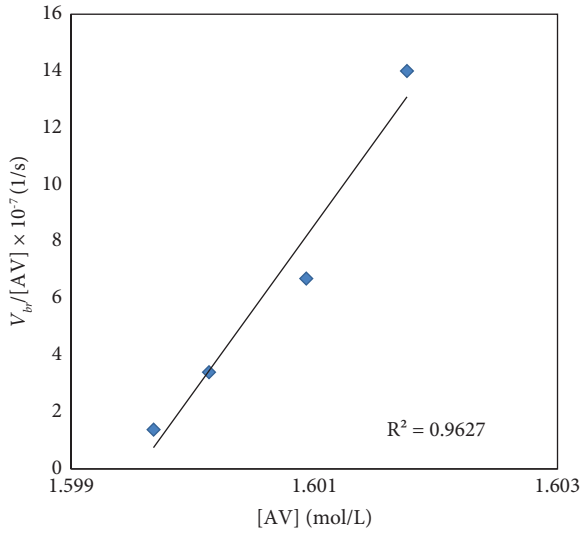

Figure 4: V_{br}/[VA] versus [VA] in dimethylformamide at X = 1.96 at 50°C.

$$I^{\cdot} + M_2 \xrightarrow{ki2} Q^{\cdot}_{0,1}, \tag{8}$$

3.3.2. Propagation

$$P^{\cdot}_{p,q} + M_1 \xrightarrow{kp11} P^{\cdot}_{p+1,q}, \tag{9}$$

$$P^{\cdot}_{p,q} + M_2 \xrightarrow{kp12} Q^{\cdot}_{p,q+1}, \tag{10}$$

$$P^{\cdot}_{p,q} + \overline{M_2M_1} \xrightarrow{kp121} P^{\cdot}_{p+1,q+1}, \tag{11}$$

$$P^{\cdot}_{p,q} + \overline{M_1M_2} \xrightarrow{kp112} Q^{\cdot}_{p+1,q+1}, \tag{12}$$

Table 1: Determination of kinetic constants of AN/VA (K_f = 0.02567) in dimethylformamide at 50°C for the estimation of CTC rate constants.

X = [AN]/[VA]	$A(X)$	$F(X)$	$(F(X)/K_f)$
1.96	0.0009	0.67	25.97
3.12	0.0011	0.82	31.87
5.37	0.0002	1.50	58.43
11.84	0.0003	2.33	90.89

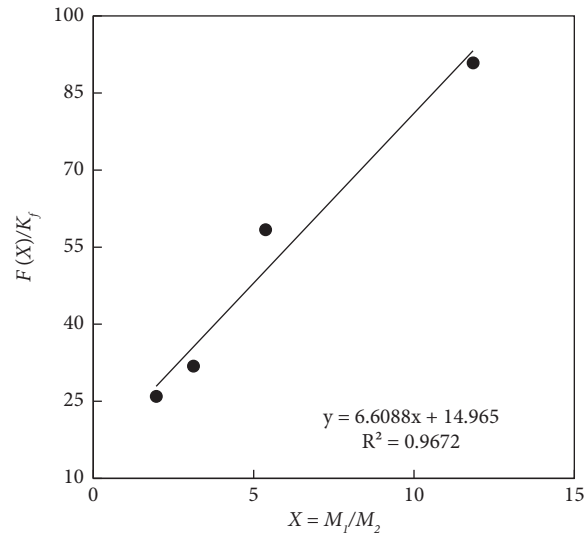

Figure 5: $F(X)/K_f$ versus X for the determination of the kinetic rate constants of the complexes.

$$Q^{\cdot}_{p,q} + M_1 \xrightarrow{kp21} P^{\cdot}_{p+1,q}, \tag{13}$$

$$Q^{\cdot}_{p,q} + M_2 \xrightarrow{kp22} Q^{\cdot}_{p,q+1}, \tag{14}$$

$$Q^{\cdot}_{p,q} + \overline{M_2M_1} \xrightarrow{kp221} P^{\cdot}_{p+1,q+1}, \tag{15}$$

$$Q^{\cdot}_{p,q} + \overline{M_1M_2} \xrightarrow{kp212} Q^{\cdot}_{p+1,q+1}. \tag{16}$$

3.3.3. Equilibrium of Complexes

$$M_1 + M_2 \overset{K_c}{\longleftrightarrow} \overline{M_1M_2}. \tag{17}$$

3.3.4. Termination

$$P^{\cdot}_{p,q} + P^{\cdot}_{s,t} \xrightarrow{kt11} P_{p+s,q+t}, \tag{18}$$

$$P^{\cdot}_{p,q} + Q^{\cdot}_{s,t} \xrightarrow{kt12} P_{p+s,q+t}, \tag{19}$$

$$Q^{\cdot}_{p,q} + Q^{\cdot}_{s,t} \xrightarrow{kt22} P_{p+s,q+t}. \tag{20}$$

3.3.5. Chain Transfer

$$P^{\cdot}_{p,q} + S \xrightarrow{ktsp} P_{p,q} + S^{\cdot}, \tag{21}$$

$$Q^{\cdot}_{p,q} + S \xrightarrow{ktsq} P_{p,q} + S^{\cdot}, \tag{22}$$

where I, M_1, and M_2 are the terms of the initiator, monomer 1, and monomer 2, respectively. The terms $I^{\cdot}$, $P^{\cdot}_{p,q}$, and $Q^{\cdot}_{p,q}$ are the free radicals when encountering the unsaturated monomers that interact with them, joining the radical as a link in a chain, making it grow. The subscripts p and q change depending on which monomer joined the chain, increasing one unit. The terms $P^{\cdot}_{1,0}$ and $Q^{\cdot}_{0,1}$ are the newly formed radicals with monomers 1 and 2, respectively. Note that $k_d, k_{ij}, k_{pjk}, k_{pjkm}, k_{tjk}$, and$k_{tsn}$ are the rate constants of dissociation, initiation, propagation of free monomers and CTCs, termination, and chain transfer.

Equations (11), (12), (15), and (16) are the terms of CTCs in the reaction mechanism that can only act on the propagation stage in this case. $\overline{M_iM_j}$ is the complex term for $i = 1$, 2 and $j = 1, 2$, where i and j cannot be equal for the complex, and CTC formation is in equilibrium, see equation (17).

3.4. Modeling of the Continuous Stirred Tank Reactor. All rate equations obtained from the reaction mechanism, equations (6)–(22), must be considered when designing the reactor. The equations obtained from the mechanism were reduced using the hypothesis of the large chain (LCH) and quasi-stationary state (QSSA). LCH states that growing chains are considerably longer; consequently, the initiator term is negligible, and the composition of the entire polymer mass is essentially the same. QSSA assumes that the termination rate is greater than the initiation rate, which minimizes the formation of new growing chains and increases the relevance of propagation velocity in the polymerization rate equations. Therefore, the terms of $P^{\cdot}_{p,q}$ and $Q^{\cdot}_{p,q}$ are reduced, and the following equations are obtained:

$$P = \sum_{p=0}^{\infty}\sum_{q=0}^{\infty} P^{\cdot}_{p,q},$$
$$Q = \sum_{p=0}^{\infty}\sum_{q=0}^{\infty} Q^{\cdot}_{p,q}, \tag{23}$$

$$\frac{dI}{dt} = -2f_i k_d I, \tag{24}$$

$$\begin{aligned}\frac{dM_1}{dt} = {} & -k_i \mathrm{IM}_1 - k_{p11} M_1 P - k_{p112}\overline{M_1M_2}P - k_{p121}\overline{M_2M_1}P \\ & -k_{p21} M_1 Q - k_{p212}\overline{M_1M_2}Q - k_{p221}\overline{M_2M_1}Q,\end{aligned} \tag{25}$$

$$\frac{dM_2}{dt} = -k_i \mathrm{IM}_2 - k_{p12} M_2 P - k_{p112}\overline{M_1M_2}P - k_{p121}\overline{M_2M_1}P - k_{p22} M_2 Q - k_{p212}\overline{M_1M_2}Q - k_{p221}\overline{M_2M_1}Q, \tag{26}$$

$$\frac{dP}{dt} = k_i \mathrm{IM}_1 + \left(k_{p21} M_1 + k_{p221}\overline{M_2M_1}\right)Q - \left(k_{p12} M_2 + k_{p112}\overline{M_1M_2}\right)P, \tag{27}$$

$$\frac{dQ}{dt} = k_i \mathrm{IM}_2 + \left(k_{p12} M_2 + k_{p112}\overline{M_1M_2}\right)P - \left(k_{p21} M_1 + k_{p221}\overline{M_2M_1}\right)Q, \tag{28}$$

$$\frac{dP_t}{dt} = -k_{t11} P - k_{t12} \mathrm{PQ} - k_{ts1} \mathrm{PS}. \tag{29}$$

Equations (24)–(26) are the rate equations for the initiator and monomers 1 and 2, respectively. All these equations were obtained from equations (6)–(22), including the terms of CTCs, which consume monomers in equations (25) and (26) and consume and generate new radicals in equations (27) and (28). The terms of equation (29) correspond to the termination steps. Consequently, equations (30) and (31) were used to calculate the concentration of the polymers with termination of M_1 and M_2:

$$P = \frac{\left(k_{p21}M_1 + k_{p221}\overline{M_2M_1}\right)Q}{\left(k_{p12}M_2 + k_{p112}\overline{M_1M_2}\right)}, \tag{30}$$

$$Q = -\left\{\frac{2fik_dI}{k_{t11}\left(k_{p21}M_1 + k_{p221}\overline{M_2M_1}/k_{p12}M_2 + k_{p112}\overline{M_1M_2}\right)^2 + 2k_{t12}\left(k_{p21}M_1 + k_{p221}\overline{M_2M_1}/k_{p12}M_2 + k_{p112}\overline{M_1M_2}\right) + k_{t22}}\right\}^{(1/2)}, \tag{31}$$

where the way in which both equations were obtained required considering the QSSA and LCH for equations (27)–(29). Note that equation (31) depends on steps of initiation and termination, where k_d, fi, and k_{tii} $(i = 1, 2)$ are the dissociation rate constant, initiator efficiency, and termination rate constant, respectively.

3.5. Reactor Design Equations. Perfect mixing was considered for the development of the CSTR model, which takes the following form:

$$\frac{dM_1}{dt} = \left(M_{1f} - M_1\right)\frac{q}{V} - \left\{\left(k_{p11}P + k_{p21}Q\right)M_1 + \left(k_{p112}P + k_{p212}Q\right)\overline{M_1M_2} + \left(k_{p121}P + k_{p221}Q\right)\overline{M_2M_1}\right\}, \tag{32}$$

$$\frac{dM_2}{dt} = \left(M_{2f} - M_2\right)\frac{q}{V} - \left\{\left(k_{p12}P + k_{p22}Q\right)M_2 + \left(k_{p112}P + k_{p212}Q\right)\overline{M_1M_2} + \left(k_{p121}P + k_{p221}Q\right)\overline{M_2M_1}\right\}, \tag{33}$$

$$\frac{dI}{dt} = \left(I_f - I\right)\frac{q}{V} - k_dI, \tag{34}$$

$$\frac{dT}{dt} = \left(T_f - T\right)\frac{q}{V} + \frac{1}{\rho Cp}\{B + C\} - \frac{hAc}{\rho CpV}\left(T - T_c\right), \tag{35}$$

$$B = \left(-\Delta H_{p11}\right)k_{p11}M_1P + \left(-\Delta H_{p12}\right)k_{p12}M_2P + \left(-\Delta H_{p112}\right)k_{p112}\overline{M_1M_2}P + \left(-\Delta H_{p212}\right)k_{p212}\overline{M_2M_1}P, \tag{36}$$

$$C = \left(-\Delta H_{p21}\right)k_{p21}M_1Q + \left(-\Delta H_{p22}\right)k_{p22}M_2Q + \left(-\Delta H_{p212}\right)k_{p212}\overline{M_1M_2}Q + \left(-\Delta H_{221}\right)k_{p221}\overline{M_2M_1}Q, \tag{37}$$

where equations (32)–(37) are the mass and energy balances of the reactor, q is the mass feed flow, V is the volume of the reactive solution, M_{if} $(i = 1, 2)$ is the feed concentration of the monomers, M_i $(i = 1, 2)$ is the concentration of monomers, I is the initiator, I_f are the feed concentrations of the initiator, T is the reaction temperature, and ΔH_{pij}, ΔH_{pijk} $(i, j, k = 1, 2)$ ρ, C_p, T_f, T_C, and $h\,A_c$ are the heat of reaction of propagation of free monomers and CTC, cooling density, heat capacity at constant pressure of cooling, feed temperature, refrigerant temperature, and dimensions of the zone of heat transfer, respectively.

The rate constants in their regular form are given by

$$k_d = k_{d0}\text{EXP}\left(\frac{-E_d}{\text{RT}}\right), \tag{38}$$

$$k_{p_{ij}} = k_{p_{ij0}}\text{EXP}\left(\frac{-E_{p_{ij}}}{RT}\right), \quad i, j = 1, 2, \tag{39}$$

$$k_{t_{\text{ii}}} = k_{t_{\text{ii0}}}\text{EXP}\left(\frac{-E_{t_{ii}}}{\text{RT}}\right), \quad i = 1, 2, \tag{40}$$

$$k_{t_{12}} = \psi\sqrt{k_{t_{11}}k_{t_{22}}}, \tag{41}$$

where $k_{d0}, k_{pij0}, and k_{tii0}$ are the dissociation rate constant, propagation rate constant, and termination rate constant at 25°C, respectively. E_d, E_{pij}, and E_{tii} $(i = 1, 2)$ are the dissociation energy, propagation energy, and termination energy, respectively, whereas R is the universal gas constant and ψ is a constant determined experimentally.

A summary of the meaning of the variables can be found in Abbreviations.

Table 2 lists the parameters used in the simulations carried out in this study [14–16]. The gel effect was not significant because of the conditions tested in the experiments. To simplify the model resolution, equations (30), (31), and (32)–(37) are dimensionless term by term, and equations (43)–(48) are the results of this mathematical reformulation. The resolution of these equation systems is totally analytical considering steady-state and gives the results in terms of various operative variables such as monomer conversion, average molecular weight, and the mole fraction of the comonomer.

3.6. Analytical Solution of the Reactor Model. This section first describes the parameters and variables used to convert equations (24)–(31) into dimensionless terms. Equations (43)–(46) correspond to the dimensionless versions of

equations (32)–(37), whose resolution process is described in detail later. The resolution for the steady state of the CSTR reactor model considers that the terms of the derivatives in equations (43)–(46) must be equal to zero. Therefore, when solving the system of equations simultaneously, this fact is considered beforehand.

To use a dimensionless formulation, the set of variables is defined [15]:

$$\tau = \frac{t}{\theta},$$

$$x_1 = \frac{M_{1f} - M_1}{M_{1f}},$$

$$x_2 = \frac{M_{2f} - M_2}{M_{2f}},$$

$$\theta = \frac{V}{q},$$

$$\mathrm{Da} = k_{p22}(T_f)\left(\frac{k_{p22}(T_f) I_f}{k_{p22}(T_f)}\right)^{1/2}\theta,$$

$$\Gamma_{21} = \frac{E_{p21}}{E_{p22}},$$

$$\Gamma = \frac{E_{p22}}{RT_f},$$

$$x_4 = \left(\frac{T - T_f}{T_f}\right)\Gamma,$$

$$r_1 = \frac{k_{p11}(T_f)}{k_{p12}(T_f)},$$

$$r_2 = \frac{k_{p22}(T_f)}{k_{p21}(T_f)},$$

$$\Gamma_{11} = \frac{E_{p11}}{E_{p22}},$$

$$y_1 = P\left(\frac{k_{p220}(T_f)}{k_d(T_f) I_f}\right)^{1/2},$$

$$\Gamma_d = \frac{E_d}{E_{p22}},$$

$$x_3 = \frac{I_f - I}{I_f},$$

$$\gamma = \frac{k_{p21}(T_f)}{k_{p12}(T_f)},$$

$$y_2 = Q\left(\frac{k_{p220}(T_f)}{k_d(T_f) I_f}\right)^{1/2},$$

$$\eta = \left(\frac{k_d(T_f) k_{t220}(T_f)}{I_f}\right)^{(1/2)} \frac{1}{k_{p22}(T_f)},$$

$$B_{11} = \frac{(-\Delta H_{p11}) M_{1f}\Gamma}{\rho C_p T_f},$$

$$B_{12} = \frac{(-\Delta H_{p12}) M_{2f}\Gamma}{\rho C_p T_f},$$

$$B_{21} = \frac{(-\Delta H_{p21}) M_{1f}\Gamma}{\rho C_p T_f},$$

$$B_{22} = \frac{(-\Delta H_{p22}) M_{2f}\Gamma}{\rho C_p T_f},$$

$$B_{112} = \frac{(-\Delta H_{p112}) M_{1f}\Gamma}{\rho C_p T_f},$$

$$B_{121} = \frac{(-\Delta H_{p121}) M_{1f}\Gamma}{\rho C_p T_f},$$

$$\Gamma_{12} = \frac{E_{p12}}{E_{p22}},$$

$$B_{212} = \frac{(-\Delta H_{p212}) M_{2f}\Gamma}{\rho C_p T_f},$$

$$B_{221} = \frac{(-\Delta H_{p221}) M_{2f}\Gamma}{\rho C_p T_f},$$

$$x_{c12} = \frac{M_{1f} - \overline{M_1 M_2}}{M_{1f}},$$

$$r_{212} = \frac{k_{p212}(T_f)}{k_{p12}(T_f)},$$

$$r_{112} = \frac{k_{p112}(T_f)}{k_{p12}(T_f)},$$

$$\Gamma_{112} = \frac{E_{p112}}{E_{p22}},$$

$$x_{c21} = \frac{M_{1f} - \overline{M_2 M_1}}{M_{1f}},$$

$$\Gamma_{212} = \frac{E_{p212}}{E_{p22}},$$

$$\Gamma_{121} = \frac{E_{p121}}{E_{p22}},$$

$$r_{221} = \frac{k_{p221}(T_f)}{k_{p21}(T_f)},$$

Table 2: Kinetic parameters used for reactor modeling.

$k_{do} = 5.95 \times 10^{13}\,\mathrm{L \cdot mol^{-1}\,s^{-1}}$ [14]	fi = 0.6 initiator efficiency [14]	$S_f = 10.49872\,\mathrm{mol \cdot L^{-1}}$
$E_d = 29.6\,\mathrm{kcal \cdot mol^{-1}}$ [14]	$T_f = T_c = 50^{\circ}\mathrm{C}$	$I_f = 0.001336\,\mathrm{mol \cdot L^{-1}}$
Monomer 1 (AN) [14]		
$k_{p110} = 3.0 \times 10^{7}\,\mathrm{L \cdot mol^{-1}\,s^{-1}}$	$E_{p110} = 6.3\,\mathrm{kcal \cdot mol^{-1}}$	$\Delta H_{p11} = 18.25\,\mathrm{kcal \cdot mol^{-1}}$
$k_{t110} = 3.0 \times 10^{15}\,\mathrm{L \cdot mol^{-1}\,s^{-1}}$	$E_{t110} = 2.8\,\mathrm{kcal \cdot mol^{-1}}$	$M_{1f} = 2.45717\,\mathrm{mol \cdot L^{-1}}$
Monomer 2 (VA) [15]		
$k_{p220} = 1.3 \times 10^{8}\,\mathrm{L \cdot mol^{-1}\,s^{-1}}$	$\mathbf{E_{p22} = 6.3\,kcal \cdot mol^{-1}}$	$\Delta H_{p22} = 21.00\,\mathrm{kcal \cdot mol^{-1}}$
$k_{t220} = 2.8 \times 10^{10}\,\mathrm{L \cdot mol^{-1}\,s^{-1}}$	$\mathbf{E_{t22} = 2.8\,kcal \cdot mol^{-1}}$	$M_{2f} = 0.2618\mathrm{mol \cdot L^{-1}}$
Copolymerization [16]		
$k_{p21}/k_{p12} = 2.93 \times 10^{2}$	$\mathbf{E_{p12} = E_{p21} = 6.3\,kcal \cdot mol^{-1}}$	$k_{p22}/k_{p21} = r_2 = 0.04$
$k_{t110}/k_{t220} = 107.14$	$\mathbf{k_{p11}/k_{p12} = r_1 = 4.05}$	

E_{p22}: propagation energy of monomer 2, E_{t22}: termination energy of monomer 2, E_{p12}: propagation energy of growing radical P with monomer 2, E_{p21}: propagation energy of growing radical Q with monomer 1, k_{p11}: propagation monomer 1 rate constant, k_{p12}: propagation growing radical P with monomer 2 rate constant, r1: copolymerization reactivity ratio 1.

$$
\begin{aligned}
\Gamma_{221} &= \frac{E_{p221}}{E_{p22}},\\
f &= \frac{M_{1f}}{M_{2f}},\\
\Gamma_{t11} &= \frac{E_{t11}}{E_{p22}},\\
\Gamma_{t12} &= \frac{E_{t12}}{E_{t22}},\\
x_{4c} &= \left(\frac{T_C - T_f}{T_f}\right)\Gamma,\\
\beta &= \frac{hA_c}{\rho C_p T_f},\\
\Gamma_{12} &= \frac{E_{p12}}{E_{p22}},
\end{aligned}
\tag{42}
$$

where $k_{pij(T_f)}$, $k_{pijk(T_f)}$, t, ΔH_{pij}, ΔH_{pijk} $(i, j, k = 1, 2)$, E_{pij}, E_{pijk}, and E_{tij} are the propagation rate constant at the feed temperature of free monomers and CTCs, operating time, heat of reaction of propagation of free monomers and CTCs, and energies of activation in propagation, CTC propagation, and termination, respectively. Other important variables are the Damköhler number (Da), the fractions y_1 and y_2 that are related with the residence time, and the radicals P and Q, respectively.

The result of applying the dimensionless variables allowed us to obtain the following equations:

$$
\begin{aligned}
\frac{dx_1}{d\tau} = &-x_1 + \mathrm{Da}\left\{(1-x_1)\left[\frac{r_1}{r_2\gamma}y_1\exp\left(\frac{\Gamma_{11}x_4}{1+x_4/\Gamma}\right) + \frac{1}{r_2}y_2\exp\left(\frac{\Gamma_{21}x_4}{1+x_4/\Gamma}\right)\right]\right.\\
&+(1-x_{c12})\left[\frac{r_{112}}{r_2}y_1\exp\left(\frac{\Gamma_{112}x_4}{1+x_4/\Gamma}\right) + \frac{r_{212}}{r_2}y_2\exp\left(\frac{\Gamma_{212}x_4}{1+x_4/\Gamma}\right)\right]\\
&\left.+(1-x_{c21})\frac{r_{121}}{r_2\gamma}y_1\exp\left(\frac{\Gamma_{121}x_4}{1+x_4/\Gamma}\right) + \frac{r_{221}}{r_2}y_2\exp\left(\frac{\Gamma_{221}x_4}{1+x_4/\Gamma}\right)\right\},
\end{aligned}
\tag{43}
$$

$$
\begin{aligned}
\frac{dx_2}{d\tau} = &-x_2 + \mathrm{Da}\left\{(1-x_2)\left[\frac{1}{r_2\gamma}y_1\exp\left(\frac{\Gamma_{12}x_4}{1+x_4/\Gamma}\right) + y_2\exp\left(\frac{x_4}{1+x_4/\Gamma}\right)\right]\right.\\
&+(1-x_{c12})\left[\frac{r_{112}}{\gamma r_2}y_1\exp\left(\frac{\Gamma_{112}x_4}{1+x_4/\Gamma}\right) + \frac{r_{212}}{r_2}y_2\exp\left(\frac{\Gamma_{212}x_4}{1+x_4/\Gamma}\right)\right]\\
&\left.+(1-x_{c21})\frac{r_{121}}{r_2\gamma}y_1\exp\left(\frac{\Gamma_{121}x_4}{1+x_4/\Gamma}\right) + \frac{r_{221}}{r_2}y_2\exp\left(\frac{\Gamma_{221}x_4}{1+x_4/\Gamma}\right)\right\},
\end{aligned}
\tag{44}
$$

$$
\frac{dx_3}{d\tau} = -x_3 + (1-x_3)\,\mathrm{Da}\,\eta \quad \exp\left(\frac{\Gamma_d x_4}{1+x_4/\Gamma}\right),
\tag{45}
$$

$$\frac{dx_4}{d\tau} = -x_4 - \beta(x_4 - x_{4c}) + B_{11}\left(x_1 + \frac{dx_1}{d\tau}\right) + B_{22}\left(x_1 + \frac{dx_1}{d\tau}\right) + \mathrm{Da}\left\{(1-x_1)\frac{y_2}{r_2}\left[B_{21}\exp\left(\frac{\Gamma_{21}x_4}{1+x_4/\Gamma}\right) - B_{11}\exp\left(\frac{\Gamma_{21}x_4}{1+x_4/\Gamma}\right)\right]\right.$$
$$+ (1-x_{c12})\frac{r_{112}}{r_2}y_1\left[B_{112}\exp\left(\frac{\Gamma_{112}x_4}{1+x_4/\Gamma}\right) - B_{11}\exp\left(\frac{\Gamma_{112}x_4}{1+x_4/\Gamma}\right) - B_{22}\exp\left(\frac{\Gamma_{112}x_4}{1+x_4/\Gamma}\right)\right]$$
$$+ (1-x_{c21})\frac{r_{121}}{r_2}y_1\left[B_{121}\exp\left(\frac{\Gamma_{121}x_4}{1+x_4/\Gamma}\right) - B_{11}\exp\left(\frac{\Gamma_{121}x_4}{1+x_4/\Gamma}\right) - B_{22}\exp\left(\frac{\Gamma_{121}x_4}{1+x_4/\Gamma}\right)\right]$$
$$+ (1-x_2)\frac{y_1}{\gamma r_2}\left[B_{12}\exp\left(\frac{\Gamma_{12}x_4}{1+x_4/\Gamma}\right) - B_{22}\exp\left(\frac{\Gamma_{12}x_4}{1+x_4/\Gamma}\right)\right] + (1-x_{c12})\frac{r_{212}}{r_2}y_2$$
$$\cdot\left[B_{212}\exp\left(\frac{\Gamma_{212}x_4}{1+x_4/\Gamma}\right) - B_{11}\exp\left(\frac{\Gamma_{212}x_4}{1+x_4/\Gamma}\right) - B_{22}\exp\left(\frac{\Gamma_{212}x_4}{1+x_4/\Gamma}\right)\right] + (1-x_{c21})\frac{r_{221}}{r_2}y_2$$
$$\left.\cdot\left[B_{221}\exp\left(\frac{\Gamma_{221}x_4}{1+x_4/\Gamma}\right) - B_{11}\exp\left(\frac{\Gamma_{221}x_4}{1+x_4/\Gamma}\right) - B_{22}\exp\left(\frac{\Gamma_{221}x_4}{1+x_4/\Gamma}\right)\right]\right\}, \tag{46}$$

$$y_1 = f y_2\left[\frac{(1-x_1)(1/r_2)\exp(\Gamma_{21}x_4/1 + (x_4/\Gamma)) + (1-x_{c21})(r_{221}/r_2)\exp(\Gamma_{221}x_4/1 + x_4/\Gamma)}{(1-x_2)(1/\gamma r_2)\exp(\Gamma_{12}x_4/1 + x_4/\Gamma) + (1-x_{c12})(r_{112}/\gamma r_2)\exp(\Gamma_{112}x_4/1 + x_4/\Gamma)}\right], \tag{47}$$

$$y_2 = \left[\frac{2f_i(1-x_3)\exp(\Gamma_d x_4/1 + x_4/\Gamma)}{(y_1/y_2)^2 r_t\exp(\Gamma_{t11}x_4/1 + x_4/\Gamma) + 2\phi(y_1/y_2)r_t^{1/2}\exp(\Gamma_{t11}x_4 + \Gamma_{t22}x_4/2\,(1+x_4/\Gamma)) + \exp(\Gamma_{t22}x_4/1 + x_4/\Gamma)}\right]^{(1/2)}, \tag{48}$$

$$\phi = \frac{k_{t12}}{\sqrt{k_{t11}k_{t22}}}, \tag{49}$$

where $x_1, x_2, x_3, x_4, x_{c12}$, and x_{c21} are the terms of conversion of monomers 1 and 2, initiator, temperature, and CTCs, $r_1, r_2, r_{112}, r_{121}, r_{212}, r_{221}$, and r_t are the reactivity ratios of monomers and CTCs, $\Gamma_{ij}, \Gamma_{tij}$, and $\Gamma_{i,j,k}$ $(i, j, k = 1, 2)$ are the activation energy ratios in propagation, termination, and CTC, and B_{ij} and B_{ijk} $(i, j, k = 1, 2)$ are the dimensionless variable relationship with heat of propagation reaction. A summary of the meaning of the variables can be found in Abbreviations.

The equations of the analytical solution were obtained in terms of monomer conversion and various operating variables. This implicit solution must be resolved as follows:

A value of x_4 is proposed considering that the chemical reaction will take place isothermally. Then, the value of x_2 is assumed to calculate x_1 following the procedure described in Appendix A. Subsequently, the values of x_1 and x_2 are used to calculate the rest of the operative variables like the Damköhler number, which is very important to define the reactor residence time. The detailed process to obtain the analytical solution of the model proposed in this study is found in Appendix A, which describes the step-by-step calculations carried out for each operative variable, as summarized in the previous paragraph.

3.7. Average Molecular Weight with the Moment Technique. Equations (50) and (51) represent the k,l-th moment for radicals $P^{\cdot}_{p,q}$ and $Q^{\cdot}_{p,q}$ and dead polymer chains $P_{p,q}$, respectively. The moments represent the concentration of polymer chains; for example, the zeroth and first moments are related to the number fraction and weight fraction molecular weight distribution of the polymer chains [17, 18]:

$$Y^A_{k,l} = \sum_{p=0}^{\infty}\sum_{q=0}^{\infty} p^k q^l \left[A^{\cdot}_{p,q}\right], \tag{50}$$

$$\lambda_{k,l} = \sum_{p=0}^{\infty}\sum_{q=0}^{\infty} p^k q^l \left[P_{p,q}\right], \tag{51}$$

where $[A^{\cdot}_{p,q}]$ and $[P_{p,q}]$ are live radical and dead polymer chain concentrations, respectively, and p and q are the number of monomers 1 and 2 added to live and dead polymer chains.

The method of the moments can be applied to the kinetic reaction of radicals $P^{\cdot}_{p,q}$ and $Q^{\cdot}_{p,q}$ (equations (27) and (28) and the dead polymers chain obtained from equations (18)–(22)). Therefore, the set of equations is shown in Appendix B and was resolved analytically in the steady state. The methodology to resolve the equations of moments was to generate a system of four equations with four unknowns from the equations given in Appendix B, which were solved simultaneously by successive substitutions [15].

The number average molecular weight is calculated using equation (52), which requires the zeroth and first moments of the dead polymer chains, while the weight average molecular weight needs the first and second moments of the dead polymer chains, as shown in equation (53):

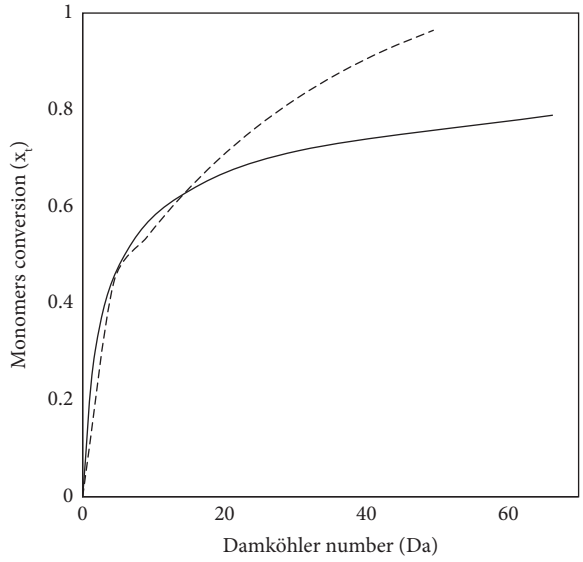

Figure 6: Comparison of conversion evolution of monomers versus the Damköhler number between the free monomer model (continuous line) and the CTC model (discontinuous line).

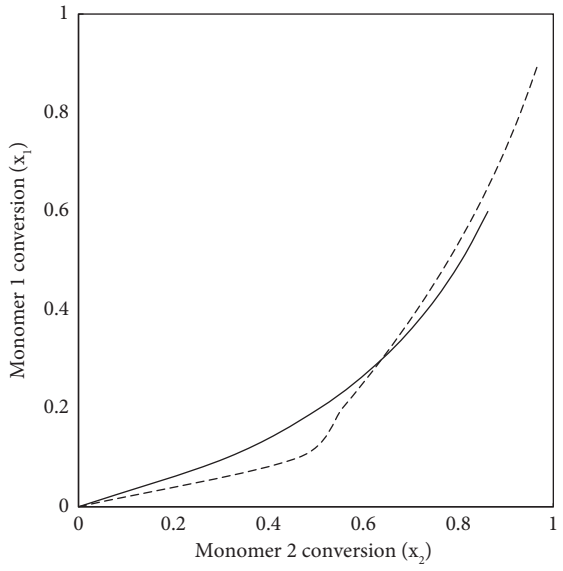

Figure 7: Comparison of variations in the conversion of monomer 1 versus monomer 2 between the free monomer model (continuous line) and the CTC model (discontinuous line).

$$\overline{M}_n = \frac{\lambda_{10} + \lambda_{01}}{\lambda_{00}}, \tag{52}$$

$$\overline{M}_w = \mathrm{MW}_1 \frac{\lambda_{20}}{\lambda_{10}} + \mathrm{MW}_2 \frac{\lambda_{02}}{\lambda_{01}}, \tag{53}$$

where MW_i ($i = 1, 2$) is the molecular weight of AN and VA and $\lambda_{00}, \lambda_{10}, \lambda_{01}, \lambda_{20}$, and λ_{02} are the zeroth, first, and second moments of dead polymer chains, respectively.

A summary of the meaning of the variables can be found in Abbreviations.

3.8. Parametric Analysis on the Influence of the Main Process Variables. The model proposed in this paper calculates some operating variables of the polymerization reactor, such as the conversion, average molecular weight, and mole fraction of the comonomer in the polymer. According to the magnitudes of these variables, the final polymer obtained had some physical and chemical properties. Parametric analysis began by defining the feed concentrations of the reactants, solvent, initiator, and reaction temperature. As discussed above, the model requires a monomer 2 conversion value to calculate the values of the other process variables. Figures 6 and 7 show the results obtained from the

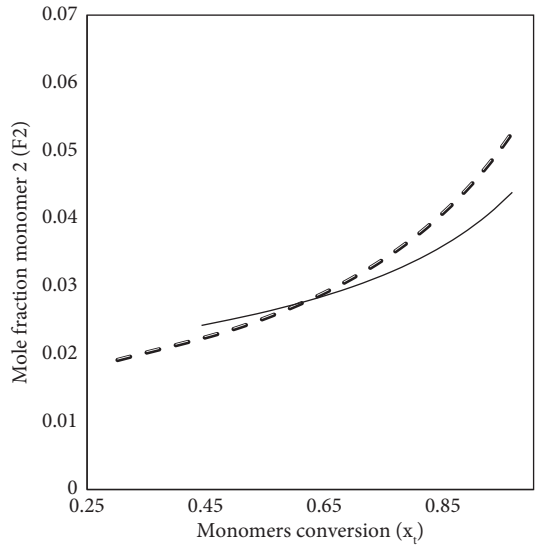

Figure 8: Comparison of mole fraction monomer 2 in polymer versus monomer conversion between the free monomer model and the CTC model.

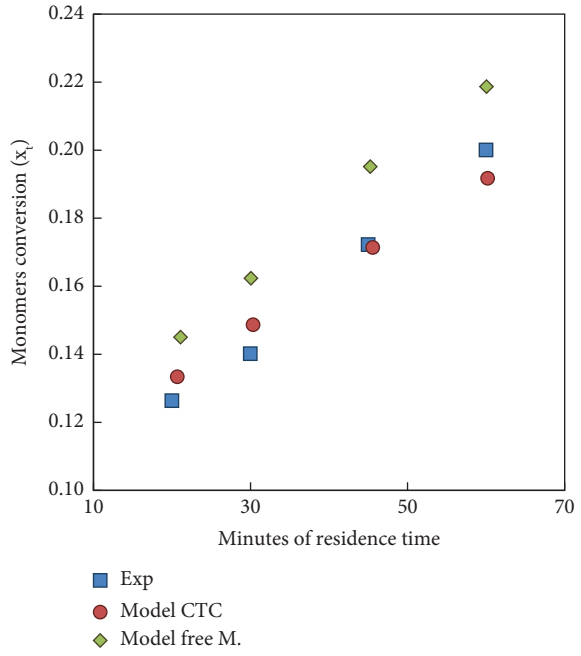

Figure 9: Comparison of experimental and predicted monomer conversions at different residence times.

analysis of the changes that occurred in various operating parameters. The continuous line is the model result for free monomer prediction, and the discontinuous line is the model prediction for CTCs.

Figure 6 shows a set of similar conversion values for Da numbers below 20. Note that the conversion of monomers changed abruptly for Da values above 20. However, in the model that considers the participation of free monomers, the change in monomer conversion is more significant than that in the model with CTCs. This indicates that the CTC model considers that monomer reactivity remains active throughout the reaction.

Figure 7 presents the variation in the conversion of monomer 1 versus that of monomer 2, where both models show similar behaviors. It should be noted that the CTC model predicts low conversions of $x1$ for $x2 = 0.6$ compared to the free monomer model. This suggests that monomer 1 at low $x2$ conversions is not sufficiently reactive.

Figure 8 shows the mole fraction of the comonomer within the polymer versus the conversion increase. A similar trend is observed for both models, suggesting that the amount of comonomer in the polymer was between 0.02 and 0.05. There is an intersection point between the predictions of both models, which indicates that there are certain

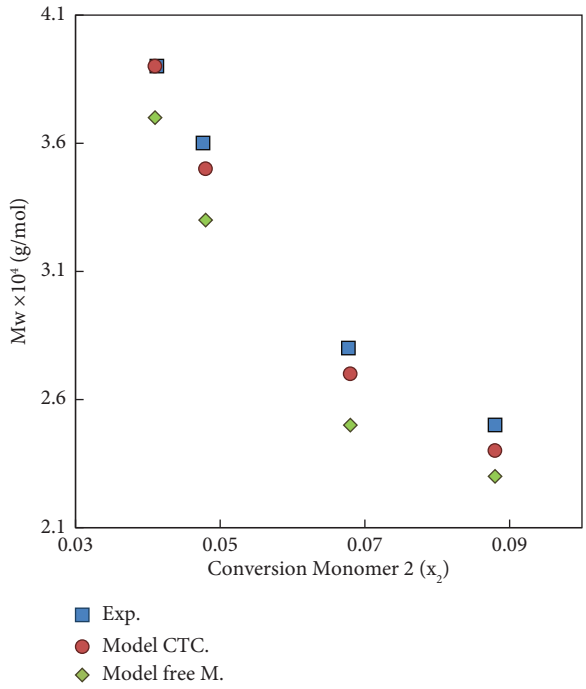

Figure 10: Comparison of experimental and predicted weight average molecular weight (Mw) versus monomer 2 conversions.

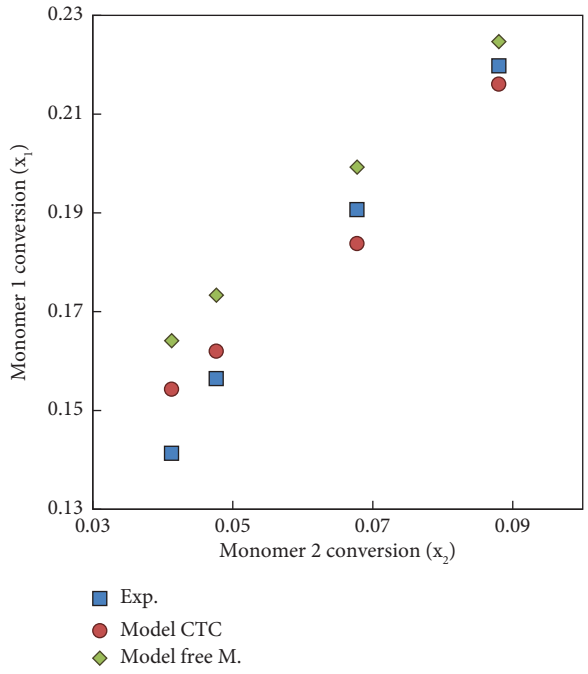

Figure 11: Comparison of experimental and predicted monomer conversion.

reactive conditions where both models achieve equal predictions.

3.9. Comparison between Model Predictions and Experimental Data. The predictions of the mathematical model were compared with the experimental test results. To validate the mathematical model, the conversion of monomers was analyzed against the minutes of the residence time, average molecular weight versus monomer conversion of 2, monomer 1 conversion versus monomer 2 conversion, and the mole fraction of monomer 2 versus monomer conversion.

The CSTR experiments achieved a steady state after three times the residence time, and each experiment was reproduced 2 times. Figure 9 shows that the total monomer conversion increases with an increase in the residence time,

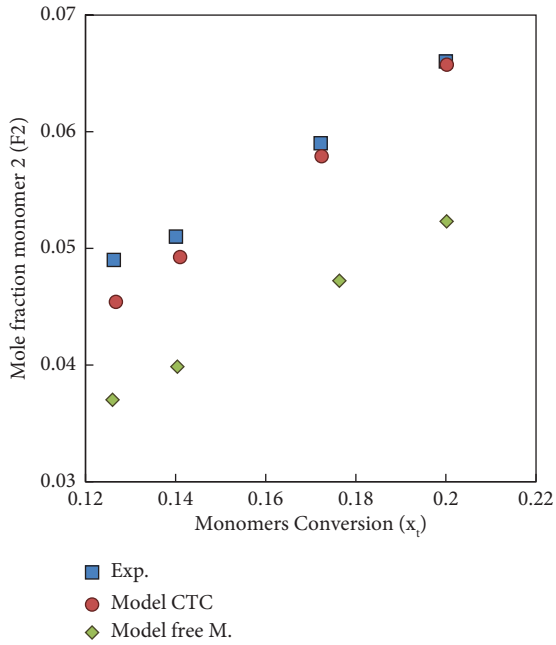

Figure 12: Comparison of experimental and predicted mole fractions of monomer 2 in the polymer formed ($F2$) versus monomer conversion.

similar to a straight line, while the simulation presents a small curvature. The experimental conversion in residence times at 20 and 30 min is below the model prediction, indicating that the model predicts more reactivity at this residence time. Figures 9 and 10 compare the model solution without considering the formation of the complexes in reaction kinetics, where the model was solved in the same way as the model involving the complexes.

As a result, the average molecular weight of the system decreased as x_2 increased. The tendency of Mw, which decreases with increasing x_2, is due to an increase in the number of active centers in the growing polymer chains, which allows the chain to be closed more easily. This is supported by the findings of Can et al. [19, 20], where they also obtained a reduction in molecular weight with the increasing comonomer amount in the polymer formed.

Figure 11 shows the changes x_1 versus x_2. The result suggests that small increases of x_1 in the first two points were associated with residence times of 20 and 30 min, while the remaining two points show x_2 changes higher than x_1 in residence times of 45 and 60 min. In agreement with these results, the increment of the residence time of monomer 2 (VA) changed its conversion faster than monomer 1 (AN).

Figure 12 shows the mole fraction of monomer 2 in polymers (F_2) versus monomer conversion (x_t), indicating that the amount of VA in the polymer formed at a specific instant. For the CTC model, a better prediction is provided regarding the experimental data, due to the effect of CTC formation on reaction kinetics.

Figures 9–12 indicate the difference between the predictions of the CTC model versus the predictions of the free monomer model, where the CTC model has better prediction than the model that does not consider CTCs.

4. Conclusions

CTC formation was observed under the experimental conditions used in this study. The charge-donor monomer would be AN, while VA would be a charge-receiving monomer owing to the electronegative tendencies of oxygen.

The rate constants of CTCs were calculated using experiments and equations (4) and (5), obtaining $k_{p121} = 1.29 \times 10^6$ and $k_{p112} = 7.81 \times 10^5$ L/mol · s at 50°C. These values have not been reported in the literature including the capacity of AN and VA to form such complexes. Moreover, calculating how fast a CTC reacts compared to the reaction rate of radicals AN and VA is possible, determining that the CTC is more reactive than free monomers, causing almost instantaneous incorporation in the polymer formed. The results of experimental CSTR copolymerization show a growing trend in monomer conversion, monomer 1 conversion vs. monomer 2 conversion, and the mole fraction of monomer 2 in the polymer formed, while the molecular weight showed a decreasing trend. The predictions of the model considering CTCs were highly reasonable in the range of interest. Furthermore, the free monomer model presents a higher error than the CTC model, implying that the improvement in the representation of the reaction mechanism considering the complexes is substantial for the analysis of this type of reactive system.

The improvements that can be focused on the model are related to more phenomena that occur in the reactive system, such as micromixing effects in the reactor and the gel effect. In addition, it is important to compare other types of models, such as the terminal model and the antepenultimate model, and to check the effects of the use of different solution systems. Also, the performance of the proposed model can

be improved by the application of dynamic data of tested reactive systems.

Appendix

A. Description of the Analytical Resolution Process of the Dimensionless Mathematical Model

The steady-state equations were solved as follows:

(i) First, the x_4 value was established due to isothermal conditions of reaction, and then, φ was defined as a variable from equation (47). We substituted it in equation (48) to obtain the next equations:

$$\varphi = \left[\frac{(1-x_1)(1/r_2) \quad \exp(x_4\Gamma_{21}/1+x_4/\Gamma) + (1-x_{c21})(r_{221}/r_2) \quad \exp(x_4\Gamma_{221}/1+x_4/\Gamma)}{\delta}\right], \tag{A.1}$$

where

$$\delta = (1-x_2)\frac{1}{\gamma r_2}\exp\left(\frac{x_4\Gamma_{12}}{1+x_4/\Gamma}\right) + (1-x_{c12})\frac{r_{112}}{\gamma r_2}\exp\left(\frac{x_4\Gamma_{112}}{1+x_4/\Gamma}\right),$$

$$y_1 = f y_2 \varphi,$$

$$\frac{y_1}{y_2} = f\varphi,$$

$$\left(\frac{y_1}{y_2}\right)^2 = f^2\varphi^2,$$

$$y_2 = \left[\frac{2f_i(1-x_3)\exp(\Gamma_d x_4/1+x_4/\Gamma)}{f^2\varphi^2 r_t \exp(\Gamma_{t11}x_4/1+x_4/\Gamma) + 2\phi\, f\varphi\, r_t^{1/2}\exp(\Gamma_{t11}x_4 + \Gamma_{t22}x_4/2\,(1+x_4/\Gamma)) + \exp(\Gamma_{t22}x_4/1+x_4/\Gamma)}\right]^{(1/2)}. \tag{A.2}$$

(ii) Substituting the new expressions for A and B in equations (43) and (44) to simplify the system of equations, the following expressions are obtained:

$$\begin{aligned} x_1 = Da\, z\{(1-x_1)[&\left[\frac{r_1}{\gamma}(f\varphi) \quad \exp\left(\frac{\Gamma_{11}x_4}{1+x_4/\Gamma}\right) + \exp\left(\frac{\Gamma_{21}x_4}{1+x_4/\Gamma}\right)\right] \\ &+ (1-x_{c12})\left[r_{112}(f\varphi) \quad \exp\left(\frac{\Gamma_{112}x_4}{1+x_4/\Gamma}\right) + r_{212}\exp\left(\frac{\Gamma_{212}x_4}{1+x_4/\Gamma}\right)\right] \\ &+ (1-x_{c21})\left[\frac{r_{121}}{\gamma}(f\varphi) \quad \exp\left(\frac{\Gamma_{121}x_4}{1+x_4/\Gamma}\right) + r_{221}\exp\left(\frac{\Gamma_{221}x_4}{1+x_4/\Gamma}\right)\right]\Big\}, \end{aligned}$$

$$x_2 = \mathrm{Da}\, z\{(1-x_2)[\left[\frac{f\varphi}{\gamma}\exp\left(\frac{\Gamma_{12}x_4}{1+x_4/\Gamma}\right)+r_2\exp\left(\frac{x_4}{1+x_4/\Gamma}\right)\right] + (1-x_{c12})\left[\frac{r_{112}f\varphi;}{\gamma}\exp\left(\frac{\Gamma_{112}x_4}{1+x_4/\Gamma}\right)+r_{212}\exp\left(\frac{\Gamma_{212}x_4}{1+x_4/\Gamma}\right)\right] + (1-x_{c21})\frac{r_{121}f\,\varphi}{\gamma}\exp\left(\frac{\Gamma_{121}x_4}{1+x_4/\Gamma}\right)+r_{221}\exp\left(\frac{\Gamma_{221}x_4}{1+x_4/\Gamma}\right)\Big\}, \tag{A.4}$$

where

$$z = \frac{1}{r_2}\left[\frac{2f_i(1-x_3)\exp(\Gamma_d x_4/1+x_4/\Gamma)}{f^2\varphi^2 r_t\exp(\Gamma_{t11}x_4/1+x_4/\Gamma)+2\phi\, f\varphi\, r_t^{1/2}\exp(\Gamma_{t11}x_4+\Gamma_{t22}x_4/2\,(1+x_4/\Gamma))+\exp(\Gamma_{t22}x_4/1+x_4/\Gamma)}\right]^{(1/2)}. \tag{A.5}$$

(iii) Daz can be eliminated from equation (A.4) by substituting using equation (A.5):

$$(1-x_1) = 1 - x_2\frac{\{A_1+B_1+C_1\}}{\{D_1+E_1+F_1\}}, \tag{A.6}$$

where

$$\begin{aligned}
A_1 &= (1-x_1)\left[\frac{r_1}{\gamma}f\varphi \quad \exp\left(\frac{\Gamma_{11}x_4}{1+x_4/\Gamma}\right)+\exp\left(\frac{\Gamma_{21}x_4}{1+x_4/\Gamma}\right)\right],\\
B_1 &= (1-x_{c12})\left[r_{112}(f\,\varphi) \quad \exp\left(\frac{\Gamma_{112}x_4}{1+x_4/\Gamma}\right)+r_{212}\exp\left(\frac{\Gamma_{212}x_4}{1+x_4/\Gamma}\right)\right],\\
C_1 &= (1-x_{c21})\left[\frac{r_{121}}{\gamma}(f\,\varphi) \quad \exp\left(\frac{\Gamma_{121}x_4}{1+x_4/\Gamma}\right)+r_{221}\exp\left(\frac{\Gamma_{221}x_4}{1+x_4/\Gamma}\right)\right],\\
D_1 &= (1-x_2)\left[\frac{f\varphi}{\gamma}\exp\left(\frac{\Gamma_{12}x_4}{1+x_4/\Gamma}\right)+r_2\exp\left(\frac{x_4}{1+x_4/\Gamma}\right)\right],\\
E_1 &= (1-x_{c12})\left[\frac{f\varphi}{\gamma}\exp\left(\frac{\Gamma_{12}x_4}{1+x_4/\Gamma}\right)+r_2\exp\left(\frac{x_4}{1+x_4/\Gamma}\right)\right],\\
F_1 &= (1-x_{21})\left[\frac{r_{112}f\varphi}{\gamma}\exp\left(\frac{\Gamma_{112}x_4}{1+x_4/\Gamma}\right)+r_{212}\exp\left(\frac{\Gamma_{212}x_4}{1+x_4/\Gamma}\right)\right].
\end{aligned} \tag{A.7}$$

(iv) Substituting φ from equation (A.1) and developing and rearranging the terms of equation (A.6), it is found that

$$x_1 = 1+\frac{b}{2a}-\frac{\left(b^2-4\mathrm{ac}\right)^{1/2}}{2a}, \tag{A.8}$$

where

$$a=\left[(1-x_2)\frac{f/r_2}{\gamma\delta}\exp\left(\frac{x_4(\Gamma_{12}+\Gamma_{21})}{1+x_4/\Gamma}\right)+(1-x_{c12})\frac{fr_{112}/r_2}{\delta}\exp\left(\frac{x_4(\Gamma_{112}+\Gamma_{21})}{1+x_4/\Gamma}\right)\right.$$
$$\left.+(1-x_{c21})\frac{fr_{121}/r_2}{\gamma\delta}\exp\left(\frac{x_4(\Gamma_{121}+\Gamma_{21})}{1+x_4/\Gamma}\right)+x_2\frac{fr_1/r_2}{\gamma\delta}\exp\left(\frac{x_4(\Gamma_{11}+\Gamma_{21})}{1+x_4/\Gamma}\right)\right], \quad (A.9)$$

$$b=-\left\{(1-x_2)\frac{f/r_2}{\gamma\delta}\exp\left(\frac{x_4(\Gamma_{12}+\Gamma_{21})}{1+x_4/\Gamma}\right)+(1-x_{c12})\frac{fr_{112}/r_2}{\delta}\exp\left(\frac{x_4(\Gamma_{21}+\Gamma_{112})}{1+x_4/\Gamma}\right)\right.$$
$$+(1-x_{c21})\frac{fr_{121}/r_2}{\gamma\delta}\exp\left(\frac{x_4(\Gamma_{121}+\Gamma_{21})}{1+x_4/\Gamma}\right)-(1-x_2)$$
$$\cdot\left[(1-x_{c12})\frac{fr_{221}/r_2}{\gamma\delta}\exp\left(\frac{x_4(\Gamma_{221}+\Gamma_{12})}{1+x_4/\Gamma}\right)+\exp\left(\frac{x_4}{1+x_4/\Gamma}\right)\right] \quad (A.10)$$
$$-x_2\left[(1-x_{c21})\frac{fr_1r_{221}/r_2}{\gamma\delta}\exp\left(\frac{x_4(\Gamma_{11}+\Gamma_{221})}{1+x_4/\Gamma}\right)+(1-x_{c12})\frac{fr_{112}/r_2}{\delta}\exp\left(\frac{x_4(\Gamma_{112}+\Gamma_{21})}{1+x_4/\Gamma}\right)+\exp\left(\frac{x_4(\Gamma_{21})}{1+x_4/\Gamma}\right)\right.$$
$$\left.+(1-x_{c21})\frac{fr_{121}/r_2}{\gamma\delta}\exp\left(\frac{x_4(\Gamma_{121}+\Gamma_{21})}{1+x_4/\Gamma}\right)\right],$$

$$c=-\left\{(1-x_2)\left\{(1-x_{c21})\frac{fr_{221}/r_2}{\gamma\delta}\exp\left(\frac{x_4(\Gamma_{12}+\Gamma_{221})}{1+x_4/\Gamma}\right)+r_2\exp\left(\frac{x_4}{1+x_4/\Gamma}\right)\right\}\right.$$
$$+(1-x_{c12})\left\{(1-x_{c21})\frac{fr_{112}r_{221}/r_2}{\delta}\exp\left(\frac{x_4(\Gamma_{112}+\Gamma_{221})}{1+x_4/\Gamma}\right)+r_{212}\exp\left(\frac{x_4\Gamma_{221}}{1+x_4/\Gamma}\right)\right.$$
$$\left.-x_2\left[(1-x_{c21})\frac{fr_{112}r_{221}/r_2}{\delta}\exp\left(\frac{x_4(\Gamma_{112}+\Gamma_{221})}{1+x_4/\Gamma}\right)+r_{212}\exp\left(\frac{x_4\Gamma_{212}}{1+x_4/\Gamma}\right)\right]\right\} \quad (A.11)$$
$$+(1-x_{c21})\left\{(1-x_{c21})\frac{fr_{121}r_{221}/r_2}{\gamma\delta}\exp\left(\frac{x_4(\Gamma_{121}+\Gamma_{221})}{1+x_4/\Gamma}\right)+r_{221}\exp\left(\frac{x_4\Gamma_{221}}{1+x_4/\Gamma}\right)\right.$$
$$\left.\left.-x_2\left[(1-x_{c21})\frac{fr_{121}r_{221}/r_2}{\gamma\delta}\exp\left(\frac{x_4(\Gamma_{121}+\Gamma_{221})}{1+x_4/\Gamma}\right)+r_{221}\exp\left(\frac{x_4\Gamma_{221}}{1+x_4/\Gamma}\right)\right]\right\}\right\}.$$

(v) Assuming a value of x_2 for the analytical solution of the equations system, it can be defined in terms of the conversion of monomers and initiators, which must be resolved simultaneously. In the present study, a degree of freedom analysis was carried out to obtain result 1. Finally, to define the system w, it was decided to assume a value of the conversion of monomer 2 to calculate x_1 from equation (A.8) and Y_2 and z' from the following expressions

$$Y_2=\eta\exp\left(\frac{\Gamma_d x_4}{1+x_4/\Gamma}\right),$$

$$z'=\frac{z}{(1-x_3)^{1/2}}. \quad (A.13)$$

(vi) The values of x_1, x_2, Y_2, and z' from equations (A.8), (A.12), and (A.13), Da and x_3 can be determined from

$$\mathrm{Da}=\frac{1+\sqrt{1+2E}}{\mathrm{EY}_2}, \quad (A.14)$$

$$x_3=\frac{\mathrm{DaY}_2}{1+\mathrm{DaY}_2}, \quad (A.15)$$

where

$$
\begin{aligned}
E &= 2\left\{\frac{z'\left[A2 + B2 + C2 + D2\right]}{x_2 Y_2}\right\}^2 \\
A2 &= \left(1 - x_2\right)\left[\frac{f\varphi}{\gamma}\exp\left(\frac{x_4\Gamma_{12}}{1 + x_4/\Gamma}\right) + r_2\exp\left(\frac{x_4}{1 + x_4/\Gamma}\right)\right], \\
B2 &= \left(1 - x_{c12}\right)\left[r_{112} f\varphi\exp\left(\frac{x_4\Gamma_{112}}{1 + x_4/\Gamma}\right) + r_{212}\exp\left(\frac{x_4\Gamma_{212}}{1 + x_4/\Gamma}\right)\right], \\
C2 &= \left(1 - x_{c21}\right)\left[\frac{r_{121} f\varphi}{\gamma}\exp\left(\frac{x_4\Gamma_{121}}{1 + x_4/\Gamma}\right)\right], \\
D2 &= r_{221}\exp\left(\frac{x_4\Gamma_{221}}{1 + x_4/\Gamma}\right).
\end{aligned}
\tag{A.16}
$$

(vii) Finally, the mole fraction of monomers AN and AV in the polymer formed (F_1 and F_2, respectively) and the total conversion x_t can be obtained from the following equations:

$$F_1 = \frac{\left[r_1 - 1\right]f_1^2 + f_1}{\left[r_1 + r_2 - 2\right]f_1^2 + 2\left[1 - r_2\right]f_1 + r_2}, \tag{A.17}$$

$$F_2 = 1 - F_1, \tag{A.18}$$

$$x_t = \frac{\left(M_{1f} - M_1\right) + \left(M_{2f} - M_2\right)}{M_{1f} + M_{2f}}, \tag{A.19}$$

where monomer 1 composition is $f_1 = (M_1/M_1 + M_2)$.

Equation (A.17) is known as the Mayo–Lewis equation and is derived from the ratio of the consumption rate of each monomer to the total monomer consumption rate. This equation is defined as the instantaneous composition and is the composition of the polymer chain during a specific time [21].

B. Equations of Moments

The expressions of first- and second-order moments of chain length for the live radical chains are given by

$$
\begin{aligned}
\frac{dY_{10}^P}{dt} &= -k_{p12}M_2Y_{10}^P - k_{p112}\overline{M_1M_2}Y_{10}^P + k_{p221}\overline{M_2M_1}Y_{10}^Q + k_{p21}M_1Y_{10}^Q - k_{t11}PY_{10}^P - k_{t12}QY_{10}^P - k_{ts1}Y_{10}^P[S], \\
\frac{dY_{01}^P}{dt} &= -k_{p12}M_2Y_{01}^P - k_{p112}\overline{M_1M_2}Y_{01}^P + k_{p221}\overline{M_2M_1}Y_{01}^Q + k_{p21}M_1Y_{01}^Q - k_{t11}PY_{01}^P - k_{t12}QY_{01}^P - k_{ts1}Y_{01}^P[S], \\
\frac{dY_{10}^Q}{dt} &= k_{p12}M_2Y_{10}^Q + k_{p112}\overline{M_1M_2}Y_{10}^P - k_{p221}\overline{M_2M_1}Y_{10}^Q - k_{p21}M_1Y_{10}^Q - k_{t12}PY_{10}^P - k_{t22}QY_{10}^Q - k_{ts2}Y_{10}^Q[S], \\
\frac{dY_{01}^Q}{dt} &= k_{p12}M_2Y_{01}^Q + k_{p112}\overline{M_1M_2}Y_{01}^P - k_{p221}\overline{M_2M_1}Y_{01}^Q - k_{p21}M_1Y_{01}^Q - k_{t12}PY_{01}^P - k_{t22}QY_{01}^Q - k_{ts2}Y_{01}^Q[S], \\
\frac{dY_{20}^P}{dt} &= -k_{p12}M_2Y_{20}^P - k_{p112}\overline{M_1M_2}Y_{20}^P + k_{p221}\overline{M_2M_1}Y_{20}^Q + k_{p21}M_1Y_{20}^Q - k_{t11}PY_{20}^P - k_{t12}QY_{20}^P - k_{ts1}Y_{20}^P[S], \\
\frac{dY_{02}^P}{dt} &= -k_{p12}M_2Y_{02}^P - k_{p112}\overline{M_1M_2}Y_{02}^P + k_{p221}\overline{M_2M_1}Y_{02}^Q + k_{p21}M_1Y_{02}^Q - k_{t11}PY_{02}^P - k_{t12}QY_{02}^P - k_{ts1}Y_{02}^P[S], \\
\frac{dY_{20}^Q}{dt} &= k_{p12}M_2Y_{20}^Q + k_{p112}\overline{M_1M_2}Y_{20}^P - k_{p221}\overline{M_2M_1}Y_{20}^Q - k_{p21}M_1Y_{20}^Q - k_{t12}PY_{20}^P - k_{t22}QY_{20}^Q - k_{ts2}Y_{20}^Q[S], \\
\frac{dY_{02}^Q}{dt} &= k_{p12}M_2Y_{02}^Q + k_{p112}\overline{M_1M_2}Y_{02}^P - k_{p221}\overline{M_2M_1}Y_{02}^Q - k_{p21}M_1Y_{02}^Q - k_{t12}PY_{02}^P - k_{t22}QY_{02}^Q - k_{ts2}Y_{02}^Q[S].
\end{aligned}
\tag{B.1}
$$

The equations for the zeroth (λ_{00}), first ($\lambda_{10}, \lambda_{01}$), and second moments ($\lambda_{20}, \lambda_{02}$) of chain length for the dead polymer chains are defined as follows:

$$\begin{aligned}
\frac{d\lambda_{00}}{dt} &= \frac{1}{2}k_{t11}P^2 + k_{t12}PQ + \frac{1}{2}k_{t22}Q^2 + \left(k_{ts1}P + k_{ts2}Q\right)[S],\\
\frac{d\lambda_{10}}{dt} &= k_{t11}PY_{10}^{P} + 2k_{t12}Y_{10}^{p}Q + k_{t22}QY_{10}^{Q} + \left(k_{ts1}P + k_{ts2}Q\right)[S],\\
\frac{d\lambda_{01}}{dt} &= k_{t11}PY_{01}^{P} + 2k_{t12}Y_{01}^{P}Q + k_{t22}QY_{01}^{Q} + \left(k_{ts1}P + k_{ts2}Q\right)[S],\\
\frac{d\lambda_{20}}{dt} &= k_{t11}\left(PY_{20}^{P} + \left[Y_{10}^{P}\right]^2\right) + 2k_{t12}\left(Y_{10}^{P}Q + Y_{10}^{P}Y_{01}^{Q}\right) + k_{t22}\left(QY_{20}^{Q} + \left[Y_{10}^{Q}\right]^2\right) + \left(k_{ts1}P + k_{ts2}Q\right)[S],\\
\frac{d\lambda_{20}}{dt} &= k_{t11}\left(PY_{02}^{P} + \left[Y_{01}^{P}\right]^2\right) + 2k_{t12}\left(Y_{20}^{Q}Q + Y_{01}^{P}Y_{01}^{Q}\right) + k_{t22}\left(QY_{02}^{Q} + \left[Y_{01}^{Q}\right]^2\right) + \left(k_{ts1}P + k_{ts2}Q\right)[S].
\end{aligned} \tag{B.2}$$

Abbreviations

$A(X)$: Constant when the monomer ratio$X$
A_c: Heat transfer area
B_{ij}: Dimensionless variable associated with the enthalpy of reaction of monomers
B_{ijk}: Dimensionless variable associated with the enthalpy of reaction of complex
b: Cell path length
C_M: Monomer acceptor concentration
C_L: Monomer donor concentration
C_p: Heat capacity at pressure cooling
Da: Damköhler number
E_d: Dissociation energy
E_{pij}: Propagation energy
E_{tij}: Termination energy
$F(X)$: Constant when the monomer ratio X
F_1, F_2: Mole fraction of monomers in polymer formed
f: Feeding ratio
f_i: Efficiency of initiator
I: Initiator concentration
$k_{1c1}\, k_{2c1}$: Rate constant of CTC
k_d: Rate constant dissociation
K_f: Equilibrium formation of CTC
k_{pij}: Propagation monomer rate constant
k_{pijk}: Propagation CTC rate constant
k_{tij}: Termination rate constant
M: Dead polymer chain
M_{1f}, M_{2f}: Feed monomer concentration
M_1, M_2: Monomer concentration
$\overline{M_1M_2}$: CTC concentration
MW_1, MW_2: Molecular weight of monomers
P, Q: Growing radicals
q: Feed mass flow
R: Universal gas constant
r_1, r_2: Copolymerization reactivity ratio
r_{ijk}: CTC reactivity ratio
S: Solvent concentration
T: Reaction temperature
t: Time
T_c: Refrigerant temperature
T_f: Feed temperature
V: Volume of reactive solution
V_{br}: Overall rate
V_{CT}: CTC rate
V_f: Free monomer rate
x_1, x_2: Monomer conversion
x_3: Initiator conversion
x_{c12}, x_{c21}: CTC conversion
x_4, x_{4c}: Dimensionless variable related to temperature of the reactor and the coolant
y_1, y_2: Dimensionless variable related to growing radicals

Greek Letters

β: Dimensionless variable related to the transfer area, heat capacity, refrigerant density, and transfer coefficient.
ΔA: Absorbance change
$\Delta\varepsilon$: Change in molar absorptivity
Γ: Dimensionless variable related to activation energy, feed temperature, and constant R
$\Gamma_d, \Gamma_{ij}, \Gamma_{tij}, \Gamma_{ijk}$: Dimensionless variables related to activation energies of the initiator, propagation, and termination of monomers and CTCs
γ: Dimensionless variable related to comonomer propagation.
η: Dimensionless variable that is related to the constant of dissociation and feeding of the initiator, propagation, and termination of monomer 2.
θ: Residence time
ρ: Density of cooling

τ: Dimensionless variable that relates the reaction time to the residence time
ψ: Constant experimentally determined.

Data Availability

The data used to support the findings of this study are available from the corresponding author upon request.

Conflicts of Interest

The authors declare that they have no conflicts of interest.

Acknowledgments

This study was supported by the National Technological of Mexico/Technological Institute of Aguascalientes under the CONACYT scholarship program.

References

[1] G. Cho, J. Jeong, M. Chae et al., "Electrochemical properties of sulfurized poly-acrylonitrile (SPAN) cathode containing carbon fiber current collectors," *Surface and Coatings Technology*, vol. 326, Part Bpp. 443–449, 2017.

[2] J. Li, C. Ding, Z. Zhang, J. Zhu, and X. Zhu, "Photo-induced reversible addition-fragmentation chain transfer (RAFT) polymerization of acrylonitrile at ambiente temperature: a simple system to obtain high-molecular-weight polyacrylonitrile," *Reactive and Functional Polymers*, vol. 1136, pp. 1–5, 2017.

[3] D. Alcalá-Sánchez, J. C. Tapia-Picazo, A. Bonilla-Petriciolet, G. Luna-Bárcenas, J. M. López-Romero, and A. Álvarez-Castillo, "Analysis of terpolymerization systems for the development of carbon fiber precursors of PAN," *International Journal of Polymer Science*, vol. 2020, Article ID 8029516, 2020

[4] H. C. Liu, C. C. Tuan, A. A. Bakhtiary-Davijani et al., "Rheological behavior of polyacrylonitrile and polyacrylonitrile/lignin blends," *Polymer*, vol. 111, pp. 177–182, 2017.

[5] N. D. Merekalova, G. N. Bondarenko, Y. I. Denisova, L. B. Krentsel, A. D. Litmanovich, and Y. V. Kudryavtsev, "Effect of chain structure on hydrogen bonding in vinyl acetate – vinyl alcohol copolymers," *Journal of Molecular Structure*, vol. 1134, pp. 475–481, 2017.

[6] P. Rivero and E. Etchechury, "Modelling the molecular weight distribution in terpolymerization systems with donor–acceptor complexes," *Computational and Theoretical Polymer Science*, vol. 11, no. 1, pp. 1–7, 2001.

[7] P. G. Rao, R. Vijayaraghavan, K. V. Raghavan, and P. S. T. Sai, "Kinetics and modeling of charge transfer polymerization of methyl methacrylate," *Asia-Pacific Journal of Chemical Engineering*, vol. 4, no. 4, pp. 495–507, 2009.

[8] P. Garra, B. Graff, F. Morlet-Savary et al., "Charge transfer complexes as pan-scaled photoinitiating systems: from 50 μm 3D printed polymers at 405 nm to extremely deep photopolymerization (31 cm)," *Macromolecules*, vol. 51, no. 1, pp. 57–70, 2018.

[9] D. Wang, P. Garra, J. P. Fouassier, B. Graff, Y. Yagci, and J. Lalevée, "Indole-based charge transfer complexes as versatile dual thermal and photochemical polymerization initiators for 3D printing and composites," *Polymer Chemistry*, vol. 10, no. 36, pp. 4991–5000, 2019.

[10] K. G. Olson and G. B. Butler, "Stereochemical evidence for the participation of a donor-acceptor complex in alternating copolymerizations. 2. Copolymer structure," *Macromolecules*, vol. 17, no. 12, pp. 2486–2501, 1984.

[11] D. A. Skoog, D. M. West, F. J. Holler, and S. R. Crouch, *Fundamentals of Analytical Chemistry*, Brooks/Cole Cengage Learning Editores, New York, NY, USA, 2014.

[12] C. Mas-Gilbert, J. Ros-Mestres, and S. Izquierdo-Aymerich, *Identificación y Diferenciación de Fibras Acrílicas por Espectroscopia Infrarroja*, Instituto de Investigación Textil y de Cooperación Industrial, Terrassa, Spain, 1971.

[13] D. Braun and F. Hu, "Free radical terpolymerization of three non-homopolymerizable monomers. Part IV. Terpolymerization of maleic anhydride, trans-anethole and vinyl-isobutylether," *Polymer*, vol. 45, no. 1, pp. 61–70, 2004.

[14] S. Fujimoto, M. Suzuki, and H. Miyama, "Vinyl copolymerization. II. Copolymerization of acrylonitrile with styrene and vinyl acetate of Japan," *Bulletin of the Chemical Society*, vol. 35, no. 1, pp. 60–63, 196.

[15] J. W. Hamer, T. A. Akramov, and W. H. Ray, "The dynamic behavior of continuous polymerization reactors—II Nonisothermal solution homopolymerization and copolymerization in a CSTR," *Chemical Engineering Science*, vol. 36, no. 12, pp. 1897–1914, 1981.

[16] J. Brandrup, *Polymer Handbook*, University Press, Cambridge, UK, 1999.

[17] E. Mastan and S. Zhu, "Method of moments: a versatile tool for deterministic modeling of polymerization kinetics," *European Polymer Journal*, vol. 68, pp. 139–160, 2015.

[18] H. Gao, I. A. Konstantinov, S. G. Arturo, and L. J. Broadbelt, "On the modeling of number and weight average molecular weight of polymers," *Chemical Engineering Journal*, vol. 327, pp. 906–913, 2017.

[19] D. S. Can, H. Baskan, S. Gumrukcu, and A. S. Sarac, "A novel carbon nanofiber precursor: poly(acrylonitrile-co-vinyl-acetate-co-itaconic acid) terpolymer," *Journal of Nanoscience and Nanotechnology*, vol. 19, no. 7, pp. 3844–3853, 2019.

[20] R. Devasia, C. P. Reghunadhan-Nair, P. Sivadasan, and K. N. Ninan, "High char-yielding poly[acrylonitrile-co-(itaconic acid)-co-(methyl acrylate)]: synthesis and properties: s," *Polymer International*, vol. 54, no. 8, pp. 1110–1118, 2005.

[21] T. Fujisawa and A. Penlidis, "Copolymer composition control policies: characteristics and applications," *Journal of Macromolecular Science, Part A*, vol. 45, no. 2, pp. 115–132, 2008.